JOURNAL OF SOLID STATE CHEMISTRY 61, 109–125 (1986)

Structure and Dynamics of Terephthalic Acid from 2 to 300 K

I. High-Resolution Neutron Diffraction Evidence for a Temperature-Dependent Order–Disorder Transition: A Comparison of Reactor and Pulsed Neutron Source Powder Techniques

P. FISCHER AND P. ZOLLIKER*

Labor für Neutronenstreuung, ETH Zürich, CH-5303 Wurenlingen, Switzerland

B. H. MEIER AND R. R. ERNST

Laboratorium für physikalische Chemie, ETH, CH-8092 Zürich, Switzerland

A. W. HEWAT

Institut Max von Laue-Paul Langevin BP 156X, F-38042 Grenoble Cedex, France

AND J. D. JORGENSEN AND F. J. ROTELLA

Argonne National Laboratory, 9700 South Cass Avenue, Illinois 60439

Received March 6, 1985; in revised form June 24, 1985

The structure of deuterated α-terephthalic acid $C_6D_4(COOD)_2$ is triclinic (low-temperature lattice constants: $a = 7.70$ Å, $b = 6.34$ Å, $c = 3.66$ Å, $\alpha = 92.98°$, $\beta = 107.88°$, $\gamma = 94.60°$, space group $P\bar{1}$). It has been refined to $R_I \sim 7\%$ from high-resolution reactor neutron powder data (D1A/ILL, Grenoble) at 2, 82, and 300 K. It has also been refined from high-resolution time-of-flight pulsed neutron source data (SEPD/IPNS, Argonne) at 15 and 80 K to $R_I \sim 6\%$. Concerning the acid hydrogen and the carbon–oxygen double bond the structure is almost fully disordered at 300 K. At low temperature there is a gradual transition to an ordered arrangement of almost linear O—D · · · O (angle = 178°) acid hydrogen bonds (O—D = 1.01 Å, D · · · O = 1.62 Å; order parameter ~1 below ~80 K). Both time-of-flight and constant wavelength data reveal a sample-contributed peak broadening which results either from strain or a small departure from the assumed structure. This systematic error in the data degrades the reliability of both the constant wavelength and time-of-flight refinements such that standard deviations of structural parameters do not overlap to the expected degree.

* Present address: Laboratoire de Cristallographie aux Rayons X, Université, CH-1211 Genève, Switzerland.

Introduction

The crystals of many carboxylic acids

0022-4596/86 $3.00

contain carboxyl dimers:

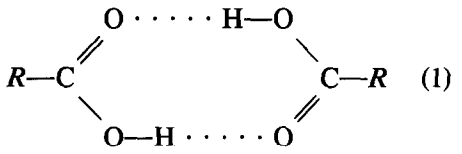

(1)

In terephthalic acid, $C_6H_4(COOH)_2$, as in several symmetrically substituted benzoic acids, orientational disorder has been observed (*1–9*). At high temperature the positions of the acidic proton as well as the carbon–oxygen single and double bonds are found to be averaged:

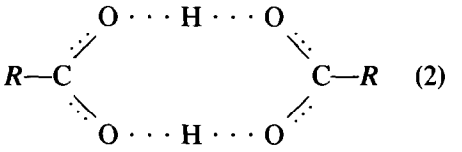

(2)

Nuclear magnetic resonance measurements on terephthalic acid (*2*) and related compounds (*2–4*) have shown, that the disorder is of a dynamic nature (see also part II). The high-temperature structure (*2*) is considered to be a rapid interchange between two tautomeric configurations:

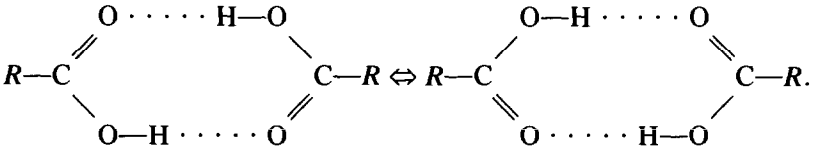

(3)

Recently (*6*), this behavior was confirmed by a quasielastic neutron scattering study. The lifetime of the tautomeric structure was found to be of the order of 10^{-10} sec at room temperature (*2, 10*). At low temperature, a transition to an ordered structure (1) may occur (*1*), as proposed for benzoic acid (*9, 10*) and *p*-toluic acid (*2*). By means of incoherent neutron scattering experiments the temperature dependence of the average mean square displacement of the carboxylic protons was determined for partially deuterated terephthalic acid (*7*).

Hydrogen order–disorder structural transitions can well be studied with neutron powder diffraction, since the isotope deuterium is a strong coherent neutron scatterer, and powder diffraction avoids problems with differently oriented domains at low temperature (*11*). (Crystal texture and twinning caused problems in a similar "single"-crystal neutron diffraction study of benzoic acid (*9*).)

Using high-resolution neutron powder diffraction the structure of deuterated α-terephthalic acid, which crystallizes in the triclinic space group $P\bar{1}$ (*12*), is investigated in the temperature range from 2 to 300 K. The results prove a gradual transition from an ordered low-temperature structure to disorder of acidic protons at high temperatures which was indicated by previous conventional neutron diffraction measurements with lower resolution (*1*). The present work compares results from both the high-flux reactor of Institut Laue-Langevin, Grenoble (spectrometer D1A) and from the Argonne intense pulsed neutron spallation source (IPNS, spectrometer, SEPD). In both cases the resolution was found to be mainly limited by sample problems.

In part II NMR results on $C_6D_4(COOH)_2$, which prove that the order–disorder transition is of dynamic nature due to an asymmetric double minimum potential, will be

discussed. Moreover the temperature dependence of the population of the two tautomeric structures is established.

Neutron Diffraction Analysis

Time-of-flight (TOF) powder techniques, using pulsed spallation neutron sources (PNS), are in principle superior to conventional reactor based neutron diffractometers: 150° backscattering permits very high resolution (*13*, *14*), and spallation sources produce more short wavelength neutrons, exciting reflexions associated with small lattice spacings (d), and thus extending the resolution of the structure (*15*). However,

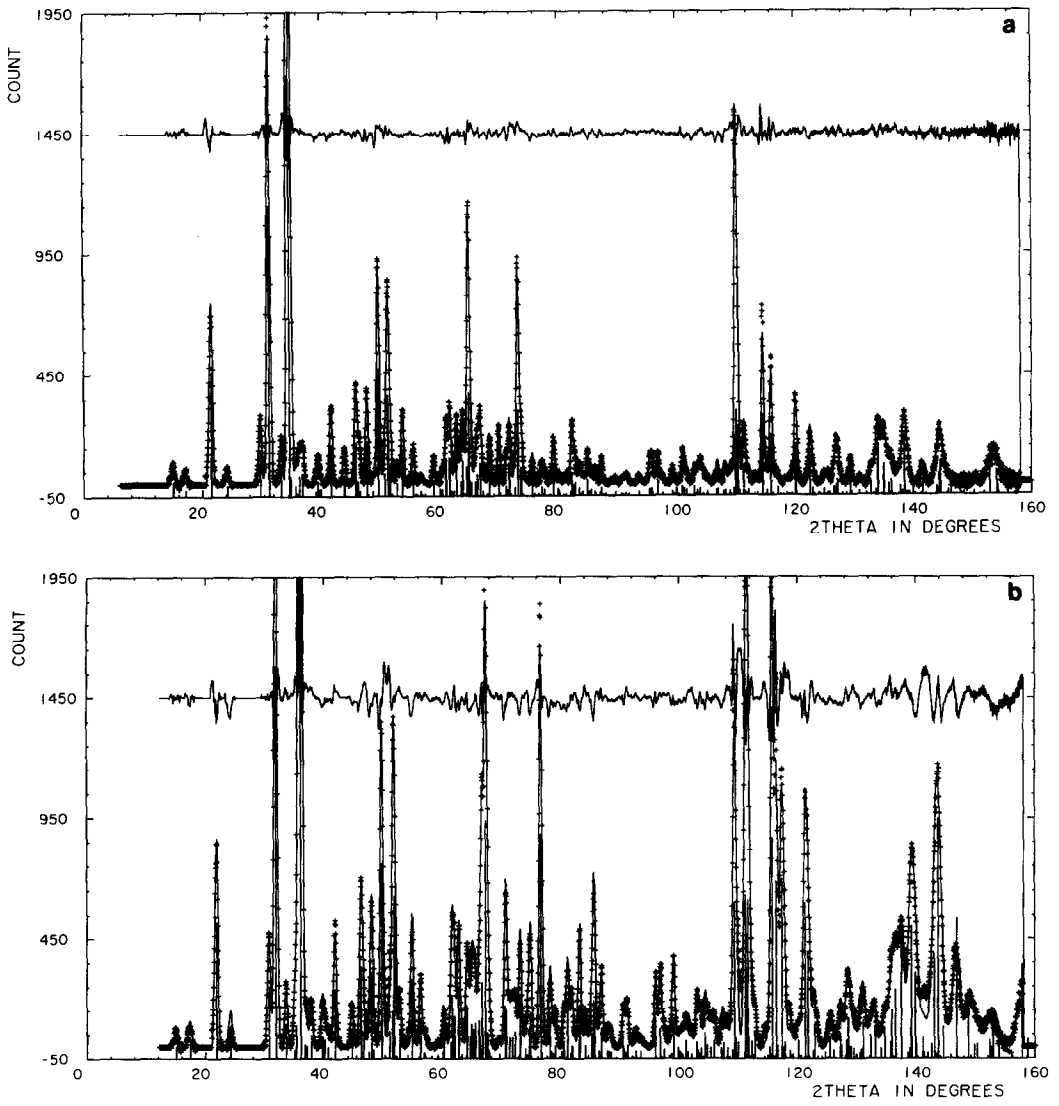

FIG. 1. Observed D1A (+) and calculated (line) neutron powder diffraction profiles of deuterated α-terephthalic acid (P = 1 bar; 1.909 Å) at (a) 300 K and (b) 2 K. The baseline bars represent the positions and structure factors of the different reflexions. The upper curves show the difference between observed and calculated intensities.

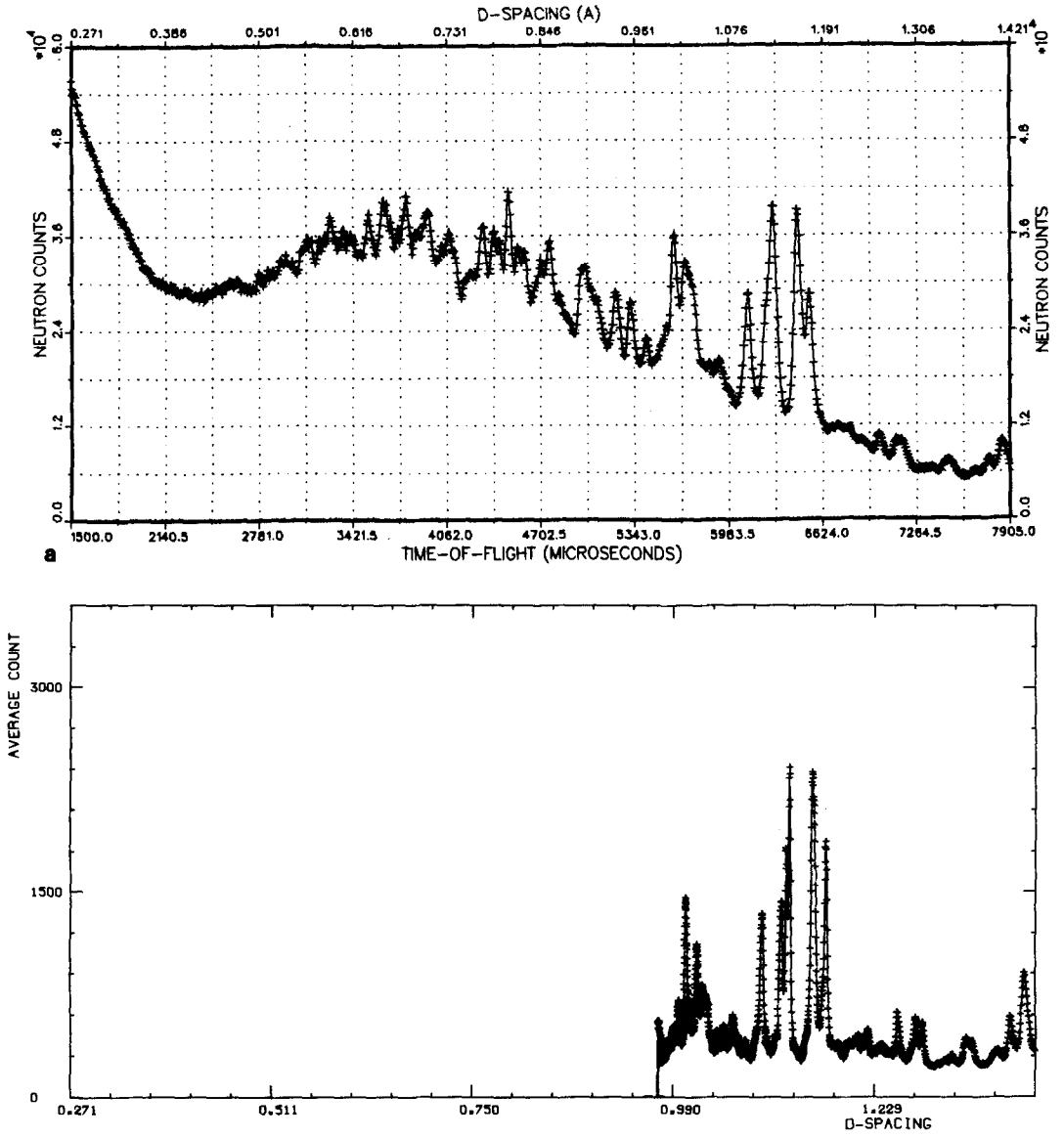

FIG. 2. (a) SEPD neutron powder diffraction profile of deuterated α-terephthalic acid at 15 K compared with (b) the D1A data at 2 K converted to the same *d*-spacing scale.

the margin of superiority may not be very large for most practical purposes (*16*); the resolution is ultimately limited by the powder sample, and, except for very simple structures, the number of reflexions increases so rapidly at short *d*-spacings that they can no longer be resolved, even using profile refinement.

Order–disorder of a hydrogen bond is just the kind of problem where the PNS-TOF technique should have a clear advantage, just as short wavelength conventional

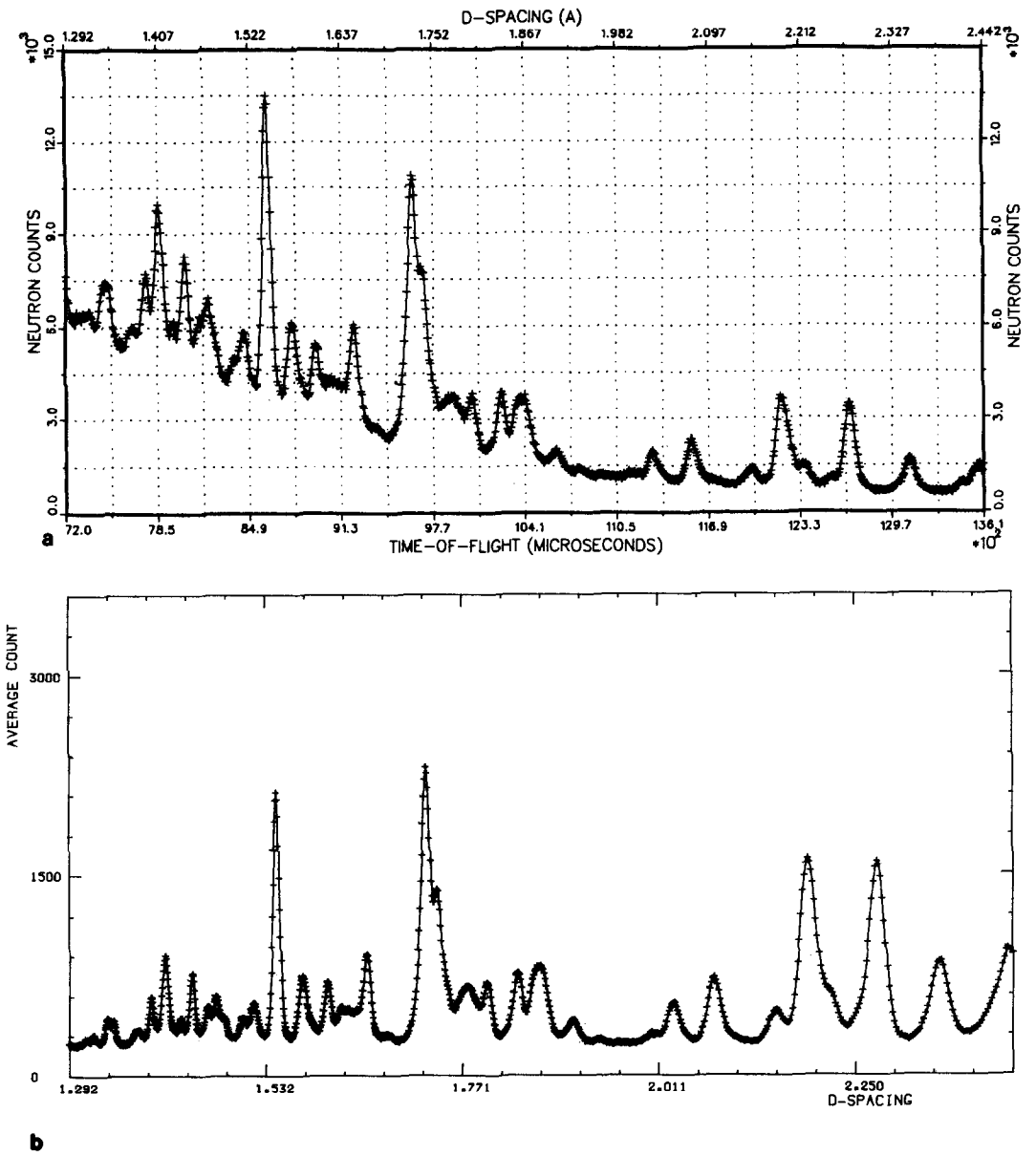

FIG. 2—*Continued.*

crystallography has an advantage for similar problems with single crystals (*17*). The new Argonne Intense Pulsed Neutron Source (IPNS) powder instruments (*14, 18–20*) are currently the best available for a practical test of the potential advantages of PNS-TOF powder techniques.

D1A Reactor Data

Dry deuterated α-terephthalic acid $C_6D_4(COOD)_2$ was sealed into a 16-mm vanadium tube. Neutron powder diffraction patterns were collected on the high-resolution diffractometer D1A at the ILL Grenoble

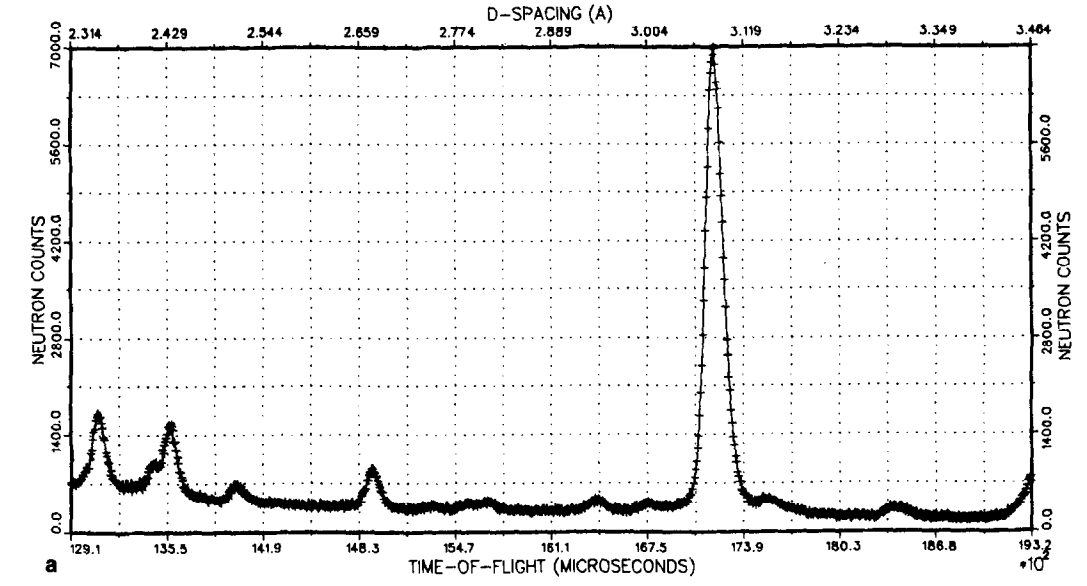

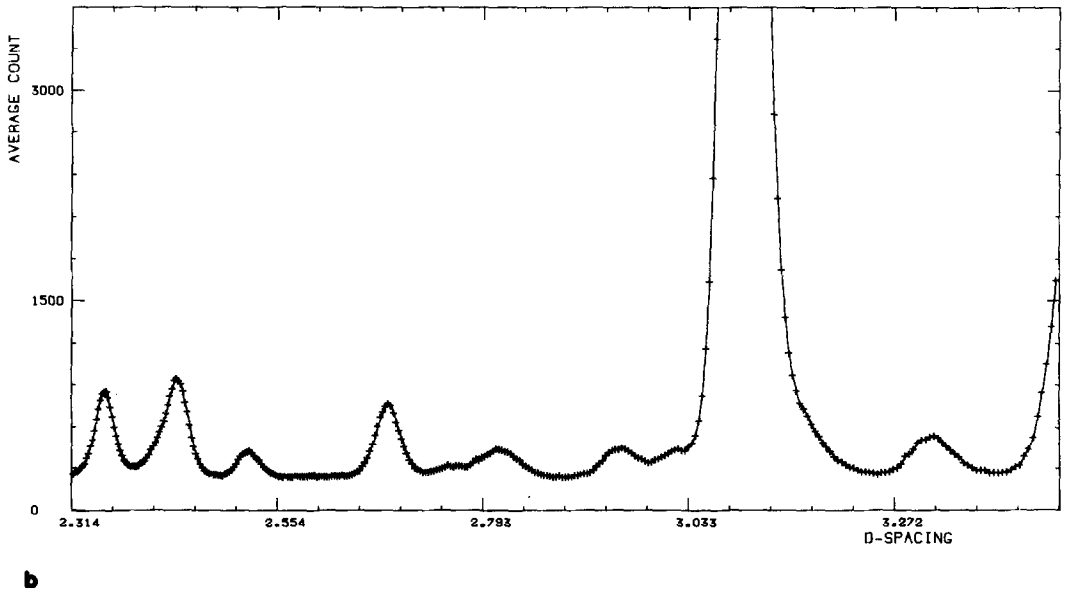

FIG. 2—*Continued.*

(*21*). The spectrometer with resolution $\Delta d/d \sim 2 \times 10^{-3}$ (d = lattice spacing) uses the scattering angle $2\theta_M = 122°$ of the monochromator and collimations $\alpha_1 \sim 19'$ (angle of reflection of the neutron guide tube) and $\alpha_3 = 10'$. Each complete scan lasted about 20 hr. The 10 counters were calibrated against one another, the average count was obtained for each point in the profile (*22*), and the temperature controlled with a helium flow cryostat. The structure was refined using the method of Rietveld (*23, 24*). Figures 1a and b show the observed and calculated profiles at 300 and 2 K, respec-

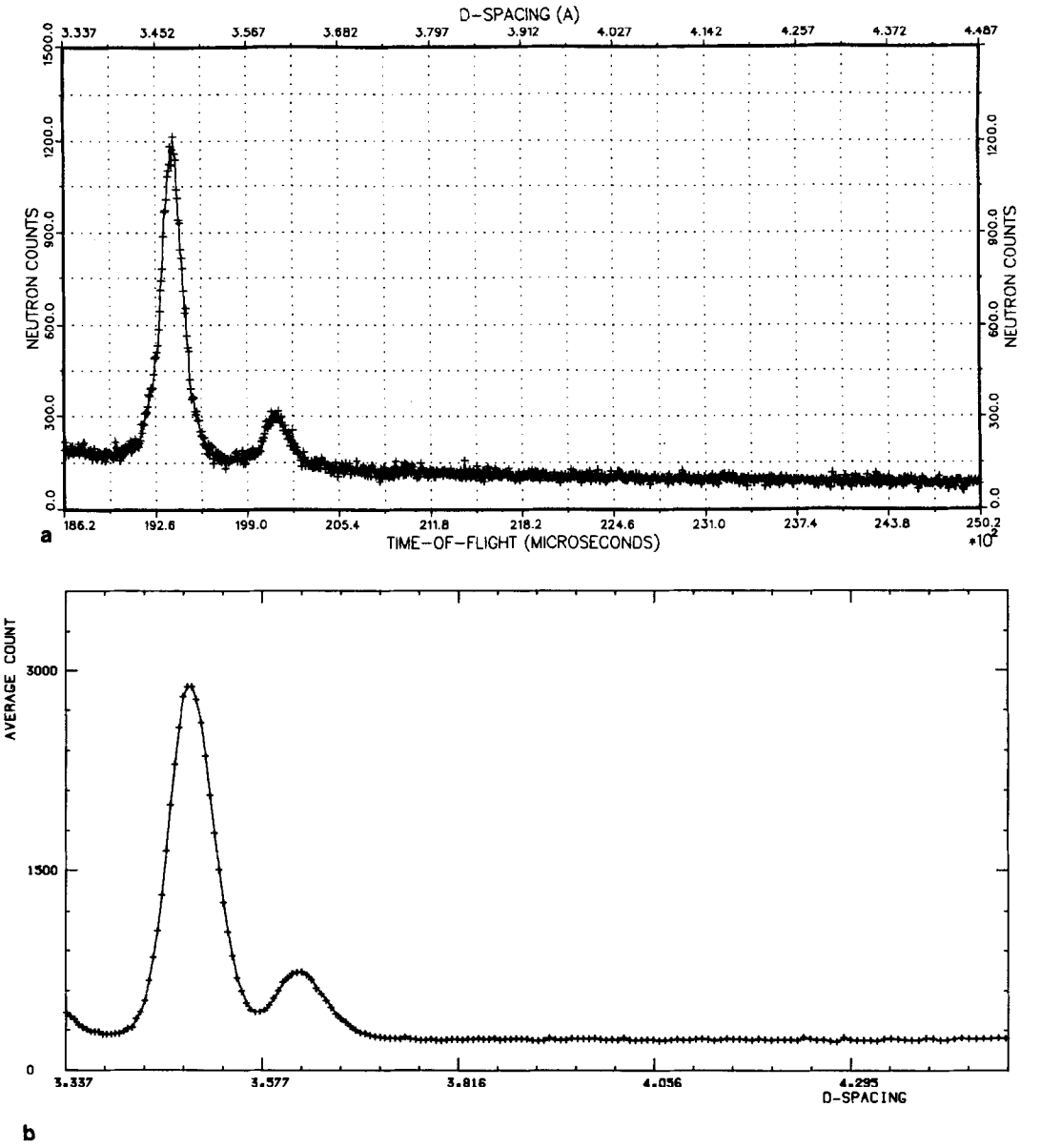

FIG. 2—*Continued.*

tively. Each pattern consists of about 3000 points (angular step 0.05°) and comprises 390 inequivalent *hkl* values.

The 82 K run, originally intended to be at 2 K, was in fact performed with a relatively large error (±10 K) near liquid-nitrogen temperature, due to a malfunction of the temperature controller. However, the actual temperature had been recorded at each data point, and this permitted the rejection of points at the beginning and end of the scan, which were further from the mean temperature. The data are nevertheless of good quality, with the only evidence of the

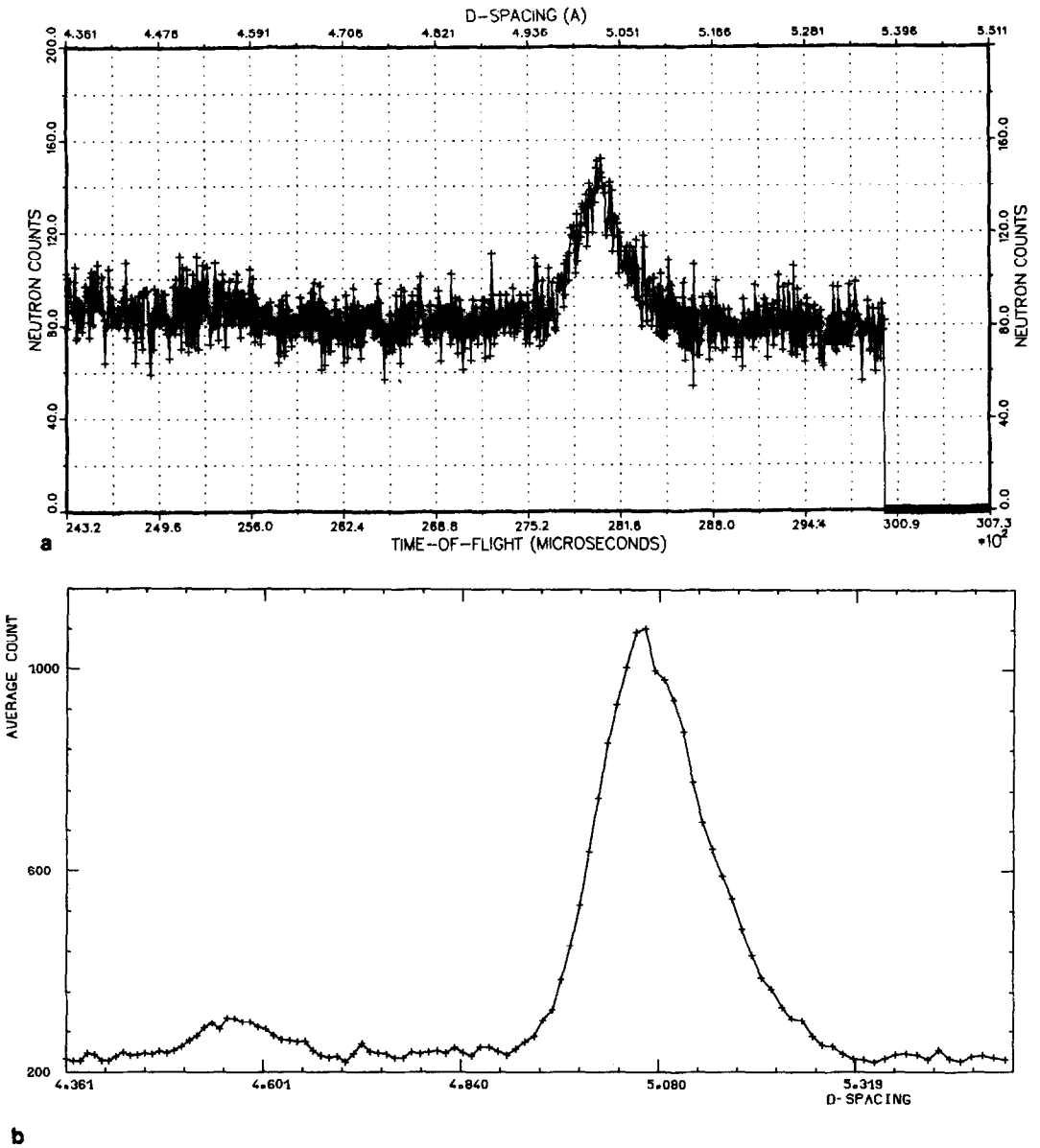

FIG. 2—*Continued.*

observed temperature variation being a slight difference between the observed and calculated line positions at high angles. The experiment was repeated, with correct temperature control at 2 K, after the TOF measurements to check the earlier results and the sample integrity.

SEPD PNS-TOF Data

The sample was repackaged in a longer but thinner (10-mm) vanadium can for the experiment on the Special Environment Powder Diffractometer (SEPD) at Argonne National Laboratory's Intense Pulsed Neu-

tron Source (IPNS) (*18, 20*). Temperatures of 80 and 15 K (the lowest conveniently obtainable) were chosen for comparison with the reactor based measurements. Data were collected for 20 hr per temperature, at scattering angles of 2θ = 150, 90, 60, 30, and 14°. Only the results for 90° scattering (Fig. 2a) were used for structural refinement because these data cover some of the larger d spacings not available in backscattering (150°). Furthermore, there is little loss of resolution at 90° because the sample shows considerable peak broadening beyond the instrumental resolution. Refinement of the high-resolution 150° data was attempted but was seriously hampered by the systematic errors resulting from not having a suitable model for the sample-contributed peak broadening. However, it was possible to learn from this analysis that the peak broadening (expressed as $\Delta d/d$) was nominally constant with a value of $\Delta d/d \sim 0.002$. The broadening must be the result of strain, stacking faults or a subtle departure from the assumed unit cell (which would require a supercell model to be invoked). Particle-size broadening is ruled out because $\Delta d/d$ is proportional to d for that case.

The constant-wavelength D1A patterns and the time-of-flight SEPD data are compared in Fig. 2 by plotting the D1A diagrams on a d-spacing scale. The D1A and SEPD data are remarkably similar. The SEPD resolution at 90° is nominally constant at $\Delta d/d = 0.005$, while D1A achieves better resolution at small d (where it is most important) and poorer resolution at large d. The better TOF resolution at large d is offset somewhat by the weaker long wavelength neutron intensity from the white beam pulsed spallation source. Thus, for both instruments, the useful range of d spacings is similar. This is disappointing, since in principle one of the chief advantages of the PNS-TOF technique should be to extend the low d-spacing range using short wavelength neutrons. In practice, for this relatively simple organic material, the rapid increase in the number of Bragg reflections and the sample contributed peak broadening limits the useful range to that available from the high-resolution diffractometer.

The rather high background in the SEPD data is the result of neutrons multiply scattered from the sample and the interior surfaces of the diffractometer. New shielding

TABLE I

LATTICE CONSTANTS, CELL VOLUMES, AND R-FACTORS FOR THIS INVESTIGATION OF DEUTERATED α-TEREPHTHALIC ACID, COMPARED TO EARLIER NEUTRON AND X-RAY REFINEMENTS OF AN UNDEUTERATED CRYSTAL (*12*)

	2 K (D1A)	15 K (SEPD)	80 K (SEPD)	82 K (D1A)	300 K (D1A)	8 K[b]	300 K[b]	X-Ray (300 K)
a (Å)	7.6966(3)[a]	7.6902(5)	7.6963(6)	7.7017(3)[a]	7.7612(2)[a]	7.699(1)	7.761(1)	7.730
b	6.3388(2)	6.3340(4)	6.3457(5)	6.3457(3)	6.4388(2)	6.336(1)	6.436(1)	6.443
c	3.6628(1)	3.6589(2)	3.6726(2)	3.6679(2)	3.7603(1)	3.660(1)	3.760(1)	3.749
α(°)	92.977(3)	92.965(5)	92.746(6)	92.919(3)	91.469(2)	92.97(1)	91.48(1)	92.75
β	107.878(3)	107.880(7)	108.060(9)	107.914(3)	109.447(2)	107.91(1)	109.54(1)	109.15
γ	94.601(2)	94.624(5)	94.772(7)	94.639(3)	95.812(2)	94.65(1)	95.84(1)	95.95
V (Å^3)	168.97(1)	168.52(1)	169.42(1)	169.47(2)	175.93(1)	—	—	—
R_P[c]	11.4	3.02	3.47	11.4	10.2	—	—	—
R_I (%)	7.7	5.27	6.84	6.9	5.9	2.9	4.5	7.5
R_{w_p}	—	5.03	5.97	—	—	7.1	8.7	—
R_e	—	1.31	1.28	—	—	3.8	4.9	—

[a] The error in the neutron wavelength (absolute distance scale) is not included in the standard deviations (in parentheses).
[b] Earlier neutron powder data (*1*).
[c] Ref (*23*).

installed inside the SEPD after these data were collected has reduced the background roughly a factor of two, making the signal-to-noise ratio on the time-of-flight diffractometer nominally equal to that on the constant-wavelength diffractometer, as it should be.

D1A Structure Refinement

The structure is assumed $P\bar{1}$ (*12*) at all temperatures, with the molecule centered at the coordinate origin. Scattering factors used were C (0.66), D (0.67), and O (0.58). That deuteration was effectively complete is indicated by the fact that neutron absorption and background scattering were both low; even a few percent of ordinary hydrogen would give noticeable contributions to both absorption and background.

Starting coordinates for Rietveld profile refinement (*23, 24*) were those obtained for Model I by Zolliker (*1*) using conventional neutron powder diffraction. Model II of Zolliker, which is simply Model I with static disorder of the (ODO) groups at high temperature, was not used. Instead, the high-temperature structure was refined with anisotropic atomic vibrational amplitudes (93 or 48 parameters for anisotropic or isotropic temperature factors, respectively); this has the advantage of assuming nothing a priori about possible disorder, which if present will in any case be dy-

TABLE II

ATOMIC COORDINATES AND AVERAGE *B* FACTORS FOR D-TEREPHTHALIC ACID (α) BETWEEN 2 AND 300 K

Atom	*x*	*y*	*z*	B_{av} (Å^2)	Atom	*x*	*y*	*z*	B_{av}
C_1	1439(9)	1478(9)	57(18)	1.70	D_1	−617(8)	3432(8)	−2911(14)	2.21
	1443(10)	1521(12)	75(23)	0.68(14)		−560(11)	3427(13)	−2853(20)	2.25(18)
	1445(14)	1539(15)	57(29)	0.60(16)		−506(13)	3422(15)	−2873(25)	1.99(20)
	1450(8)	1474(9)	138(17)	1.35		−637(8)	3457(9)	−2902(14)	2.59
	1482(10)	1457(11)	48(16)	2.25(2)		−589(9)	3442(10)	−2861(14)	2.83(3)
C_2	−314(6)	1902(8)	−1576(16)	1.07	D_2	3221(7)	−876(9)	3039(16)	2.39
	−351(8)	1912(11)	−1585(21)	0.92(15)		3251(8)	−881(12)	3039(20)	1.31(18)
	−342(11)	1838(12)	−1578(22)	0.40(15)		3245(14)	−996(18)	3013(31)	2.32(23)
	−320(7)	1936(9)	−1573(16)	1.30		3219(8)	−868(9)	3100(16)	2.18
	−336(8)	1904(8)	−1650(18)	2.19(2)		3252(9)	−817(10)	3023(16)	3.71(3)
C_3	1728(7)	−471(8)	1612(14)	0.56	O_1	4606(8)	2484(9)	1924(16)	0.94
	1826(9)	−429(10)	1599(19)	0.25(13)		4608(12)	2495(14)	1876(24)	1.33(19)
	1900(12)	−390(10)	1616(24)	0.13(16)		4569(13)	2517(14)	1840(26)	0.23(16)
	1748(8)	−450(8)	1667(14)	0.71		4627(10)	2507(10)	1873(17)	1.41
	1801(8)	−441(8)	1755(15)	1.87(2)		4601(10)	2583(9)	1799(20)	2.37(3)
C_4	3016(8)	3016(10)	60(16)	1.39	O_2	2752(8)	4661(10)	−1678(16)	1.27
	3025(10)	3045(14)	68(21)	1.31(16)		2736(10)	4610(12)	−1835(20)	0.98(14)
	3005(15)	3095(20)	64(32)	2.57(28)		2783(13)	4659(18)	−1906(30)	1.87(25)
	3001(9)	2994(11)	76(16)	1.84		2726(9)	4649(10)	−1754(17)	1.71
	3008(8)	3022(9)	77(20)	2.37(3)		2651(9)	4617(9)	−1778(19)	2.57(3)
					D_3	5605(8)	3583(10)	1752(17)	2.84
						5635(11)	3577(14)	1721(22)	2.17(14)
						5684(14)	3642(20)	1701(31)	2.37(20)
						5635(9)	3610(11)	1766(17)	3.28
						5824(16)	3930(18)	1658(21)	5.29(4)

Note. The order of entries is D1A (2 K), SEPD (15 K), SEPD (80 K), D1A (82 K), D1A (300 K). Coordinates are multiplied by 10^4. At 300 K, anisotropic B_{ij} factors were needed to describe the dynamic disorder in the structure, especially for the deuterium atom (Fig. 3); they have been averaged (B_{av}) in this table.

TABLE III

BOND LENGTHS AND ANGLES IN D-TEREPHTHALIC ACID (α) BETWEEN 2 AND 300 K

Bond (Å) Angle (°)	D1A (2 K)	SEPD (15 K)	SEPD (80 K)	D1A (82 K)	D1A (300 K)
C_1—C_2	1.353(8)	1.375(10)	1.353(14)	1.377(8)	1.405(9)
C_1—C_3	1.393(8)	1.397(11)	1.401(13)	1.376(8)	1.401(9)
C_1—C_4	1.494(9)	1.492(12)	1.489(17)	1.480(10)	1.472(10)
C_2—C_3	1.356(8)	1.412(10)	1.445(13)	1.380(8)	1.390(8)
C_2—D_1	1.118(7)	1.090(11)	1.132(13)	1.114(8)	1.109(8)
C_3—D_2	1.163(7)	1.128(10)	1.113(14)	1.152(8)	1.122(9)
C_4—O_1	1.286(8)	1.280(12)	1.272(16)	1.294(10)	1.255(9)
C_4—O_2	1.248(9)	1.236(12)	1.248(18)	1.272(10)	1.259(9)
O_1—D_3	1.014(9)	1.020(13)	1.078(16)	1.014(10)	1.235(14)
O_2—D_3	1.624(9)	1.619(12)	1.519(16)	1.610(10)	1.420(14)
C_2—C_1—C_3	117.9(6)	119.6(7)	119.5(9)	119.4(5)	119.3(6)
C_2—C_1—C_4	121.1(5)	122.4(7)	123.7(9)	119.4(5)	119.1(6)
C_3—C_1—C_4	121.0(5)	117.8(7)	116.6(9)	121.0(5)	121.6(6)
C_1—C_2—C_3	120.3(5)	121.4(7)	125.7(8)	118.6(5)	120.2(5)
C_1—C_2—D_1	120.6(6)	116.2(7)	112.0(9)	122.3(6)	119.4(6)
D_1—C_2—C_3	119.2(5)	122.4(7)	122.2(8)	119.0(6)	120.4(6)
C_1—C_3—C_2	121.8(5)	118.9(6)	114.5(8)	122.0(5)	120.5(5)
C_1—C_3—D_2	119.3(6)	124.5(7)	132.1(10)	120.4(6)	119.1(6)
D_2—C_3—C_2	118.8(5)	116.5(7)	113.3(9)	117.6(5)	120.2(6)
C_1—C_4—O_1	114.8(6)	114.9(8)	113.3(11)	116.3(6)	116.3(6)
C_1—C_4—O_2	120.7(5)	119.3(7)	122.2(10)	121.0(6)	119.0(6)
O_1—C_4—O_2	124.5(6)	125.6(9)	123.9(12)	122.7(7)	124.6(7)
C_4—O_1—D_3	110.3(7)	111.4(10)	112.3(11)	113.0(7)	113.4(8)
C_4—O_2—D_3	123.4(5)	122.0(7)	123.5(9)	122.7(6)	116.6(7)
O_1—D_3—O_2	177.5(6)	175.0(10)	173.0(13)	178.0(7)	174.5(9)

Note. At high temperature, the bonds C_4—$O_1 \cdots D_3$ and C_4'—$O_2 \cdots D_3$ are nearly equivalent, while at low temperature, the acid hydrogen D3 is strongly bonded to O_1 and hydrogen bonded to O_2, which apparently accepts the double bond with C_4.

namic, and indistinguishable from a half-atom model at this resolution (*17*). The results of the profile refinements yielding the agreement values $R_I \sim 7\%$ are summarized in Fig. 1, Tables I and II. Table III and Fig. 5 contain corresponding interatomic distances.

In the present case the resolution of the spectrometer ($\Delta d/d \sim 2 \times 10^{-3}$) could not be fully used, as the organic powder sample limited $\Delta d/d$ to $\sim 4 \times 10^{-3}$ at the lattice spacing $d \sim 1.1$ Å. The 2 K diffraction patterns (see Fig. 1) indicates noticeable deviations between calculated and observed intensities, particularly in the scattering angle range $2\theta \sim (108\text{–}120)°$. A preferred orientation correction corresponding to reciprocal lattice vector 110 improved the fit with isotropic temperature factors to $R_{w_p} = 0.135$, $R_p = 0.106$, $R_I = 0.058$, and $R_e = 0.067$, but the overall picture of the fit remains about the same. The larger observed intensity at $2\theta \sim 116°$ could be due to an impurity (e.g., a high-temperature phase, see (*12*)), stacking faults or a minor inconsistency of the structure model. However no superstructure peaks were observed. Attempts with other unit cells did not improve the fits based on Gaussian peak shape significantly. Because of the mentioned problems, the systematic errors certainly exceed the standard deviations of parameters given in Ta-

bles I to III. Nevertheless $R_I \sim 6$ to 8% suggests that the essential features of the structure are correct, but we do not exclude the possibility of improvements in further experiments or sample preparation.

The ORTEP (*25*) plot of the *z*-axis projection of this model at 300 K (Fig. 3a) clearly shows evidence for a strong disorder. The thermal ellipsoid for the acid hydrogen has large amplitudes, with the major axis along the O · · · D · · · O bonds. This ellipsoid is effectively centered between these oxygen atoms, which are then virtually equivalent. In Table III, the bonds C_4—O_1 · · · D_3 and C_4'—O_2 · · · D_3 are nearly equal at 300 K, while at 82 and 2 K, $C_4 = O_2$ is shorter than C_4—O_1, and O_1 has "captured" the acid hydrogen ion D_3. These different bond lengths (or strengths) can be represented as

300 K:

$$C_4 \cdots O_1 \cdots D_3 \cdots O_2 \cdots C_4',$$

82 K, 2K:

$$C_4—O_1—D_3 \cdots O_2 = C_4'.$$

C_4—O_1 now has the length expected for a carbon–oxygen single bond, but C_4'=O_2 is still a little too long for an isolated carbon–oxygen double bond.

The ORTEP plot of the *z*-axis projection at 2 K (Fig. 3b) shows how the center of this acid hydrogen distribution is now strongly displaced toward O_1 and away from O_2. Even at 300 K, however, there is a small displacement of D_3 from the center of (O_1, O_2), which could indicate that disorder is not complete.

SEPD PNS-TOF Structure Refinement

The time-of-flight data were also refined by the Rietveld technique (*26*) with isotropic thermal motion for all atoms at 15 and 80 K. As an example the observed and calculated profiles at 15 K are shown in Fig. 4. The largest problems in the fit occur in the same regions as for the D1A data. The TOF results, which are included in Tables I–III, confirm that D_3 is bonded to O_1, even though at 80 K the O_1—D_3 distance is found to be several standard deviations longer. This distance is of course strongly dependent on temperature. Again, the TOF results agree with C_4 being slightly closer to O_2 than to O_1, consistent with C_4=O_2 and C_4—O_1 bonds. The lattice parameters do not agree perfectly with the reactor based diffractometer results.

The difference in refined lattice constants and atomic parameters is a result of the fact that the model describes the data only approximately. Thus, the parameter estimates are biased differently for the two different techniques, and the standard deviations underestimate the uncertainties in the structure (*27*). Because of these problems in the data, it was not surprising that attempts to refine the TOF data with anisotropic temperature factors were unsuccessful. In general, the refinement was not stable enough to converge, or else yielded nonpositive definite thermal ellipsoids, or both. Attempts to refine anisotropic *B*'s for only those cases for which *B* isotropic was greater than 1.0 led to similar problems.

There remains the possibility that the $P\bar{1}$ structural model is not quite correct. An incorrect unit cell or stacking faults might explain the lack of refinement stability, peak broadening, and different answers obtained by the two techniques. However, no extra supercell peaks could be identified in either the constant-wavelength or time-of-flight data.

Bond Lengths and Angles

It is instructive to examine the bond lengths and angles summarized in Table III, since we have several independent sets of data. The determined values correspond reasonably to those known for other carboxylic acids, see, e.g., (*8, 9*) and the re-

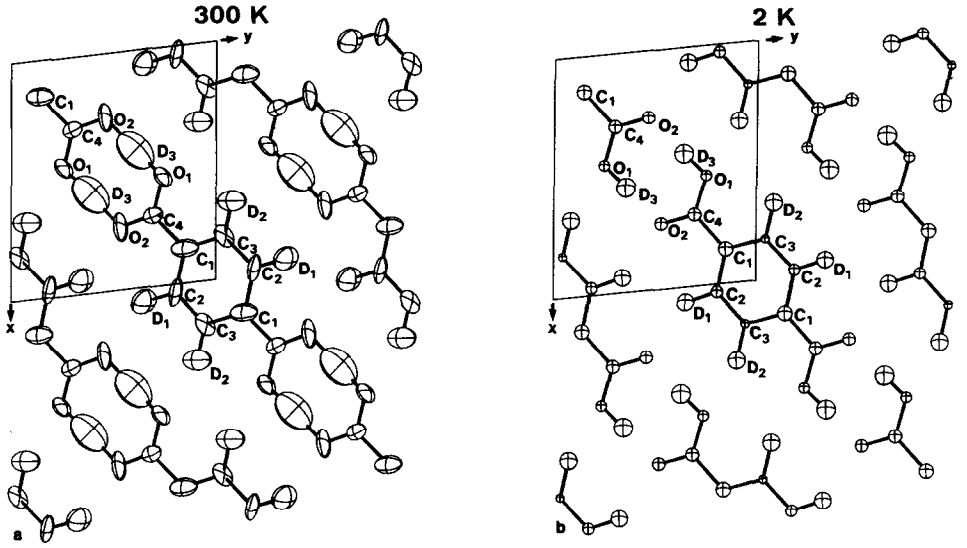

FIG. 3. ORTEP plots of the crystal structure of deuterated α-terephthalic acid projected along the z axis at (a) 300 K and (b) 2 K. At high temperature, the acid hydrogen D3 (large ellipsoid) is disordered between the essentially equivalent oxygens O_1 and O_2 of adjacent molecules; at low temperature, D3 is ordered close to O_1 and far from O_2, which are then no longer equivalent, O_2 presumably forming the double bond with C_4.

view published by Leiserowitz (*5*). First of all, we might expect the bonds C_1—C_2, C_1—C_3, and C_2—C_3 to be chemically equivalent and a different bond length C_1—C_4 because C_4 is bonded to the oxygens (see Figs. 3, 5). Indeed this is verified to within approximately the calculated errors for the D1A data at all temperatures, and also for the 15 K SEPD data (Fig. 5). The spread in the results for the 80 K SEPD data is larger than the spread in the D1A results. Similar conclusions apply for the C—C—C bond angles, with the results falling around the ideal value of 120°. The larger spread of the 80 K SEPD data is probably due to a different influence of line-broadening effects.

Both methods yield similar C—O and C—D distances. At low temperatures the approximately linear hydrogen bond O—D · · · O of D_3 (angle 178°) is short to O_1: 1.01 Å and considerably longer to O_2: 1.62 Å. However, at 300 K the acidic protons are almost disordered (O_1—D_3 = 1.24 Å, O_2—D_3 = 1.42 Å). Finally with respect to the NMR investigations (see part II) the minimum D3—D3 distance of 2.349(9) Å at 2 K is of interest.

Conclusion

Without assuming any particular model for disorder in triclinic α-terephthalic acid, we have shown that at 300 K the acid hydrogen is almost disordered (~70% based on distance arguments) between effectively equivalent O_1 and O_2 carboxyl oxygens. This indicates two nearly equivalent configurations of the (COOD) groups. At temperatures below approximately 80 K the structure becomes ordered with two localized OD groups (order parameter ~1, in fair agreement with part II). However, the degree or ordering increases slowly with decreasing temperature. The gradual change is evident from the temperature dependence of the order parameter given in part II.

In this practical example of powder dif-

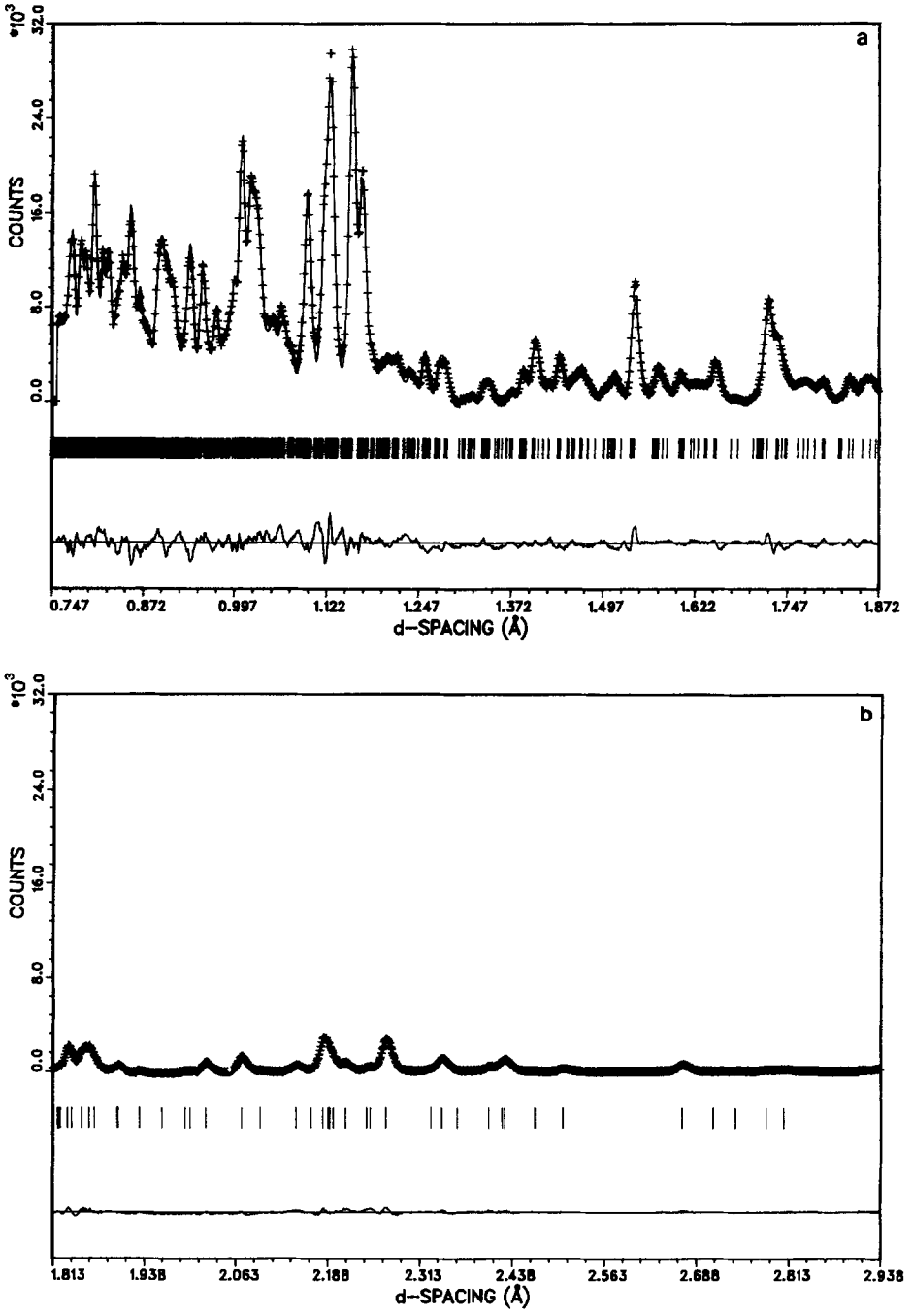

FIG. 4. Observed (+) and calculated (solid line) SEPD neutron powder diffraction profiles for deuterated α-terephthalic acid. Thick marks below the data indicate the positions of allowed Bragg reflexions used in the calculation. A difference curve (observed minus calculated) appears at the bottom. Background was fitted as part of the refinement, but has been subtracted before plotting. ($C_6D_4(COOD)_2$, 15 K (SEPD, $2\theta = 90°$): triclinic $P\bar{1}$ (isotropic B's).)

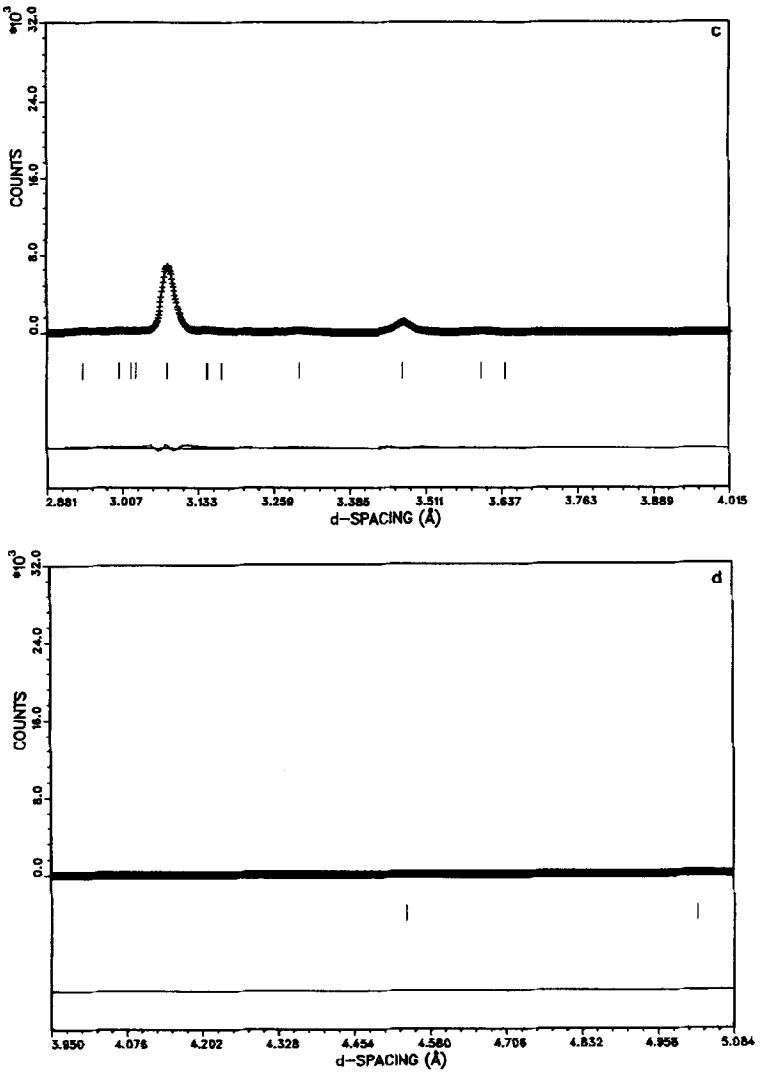

FIG. 4—*Continued.*

fraction from a simple organic material, the natural line broadening from the sample was found to be important. The resolution in the diffraction profile was therefore determined by the sample, and not by the diffractometer. Thus the theoretical advantage of backscattering TOF geometry could not be realized. Indeed, to avoid the effects of peak broadening and to obtain the larger *d* spacings, which could not be reached with 150° TOF geometry, it was necessary to use only the lower resolution 90° scattering data. This experience suggests that, in general, future Rietveld refinement codes for time-of-flight data should include the provision for simultaneously refining data from more than one scattering angle. This would allow the data to be extended over a large range of *d* spacings with the high-resolution backscattering data being used only at small *d* spacings where observed intensities are high. In the case of the present or-

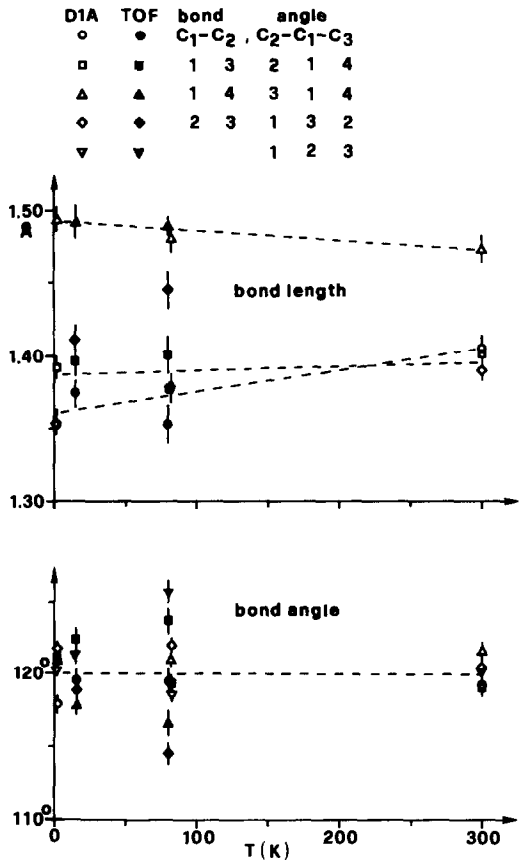

FIG. 5. Temperature dependences of C—C bond lengths and C—C—C bond angle distributions of deuterated α-terephthalic acid. D1A and TOF denote constant-wavelength and time-of-flight results, respectively. The dashed lines are guides to the eye.

ganic compound sample problems have made a comparison of the constant-wavelength and time-of-flight techniques of limited value, since the inadequacy of the model in fitting the data leads to parameter estimates which are biased differently in each case. The cause of these problems remains to be determined in future experiments. Even though this prevents the study of some of the fine details of the structure, important general conclusions about the ordering of the acid hydrogen are clearly supported by all of the data. The transition from an ordered low-temperature structure to disorder at high temperatures is gradual, i.e., does not correspond to a classical order–disorder phase transition with well defined transition temperature T_c. As will be shown in part II by means of NMR results, the disorder is of dynamic origin due to double proton exchange associated with an asymmetric double minimum potential.

Acknowledgments

We thank Dr. A. Furrer, Professor W. Hälg, and A. Stöckli for support and stimulating discussions. The authors acknowledge the U.S. Department of Energy for supporting the neutron diffraction measurements at the Intense Pulsed Neutron Source which is operated as a user facility.

References

1. P. ZOLLIKER, "Neutronenspektroskopische Untersuchung der Dynamik verschiedener Carboxylsäuren," report AF-SSP-121, Institut für Reaktortechnik, Eidg. Technische Hochschule, Zurich (1982).
2. B. H. MEIER, F. GRAF, AND R. R. ERNST, *J. Chem. Phys.* **76,** 767 (1982).
3. S. NAGAOKA, T. TERAO, F. IMASHIRO, A. SAIKA, N. HIROTA, AND S. HAYASHI, *Chem. Phys. Lett.* **80,** 580 (1981).
4. S. NAGOAKA, T. TERAO, F. IMASHIRO, A. SAIKA, N. HIROTA, AND S. HAYASHI, *J. Chem. Phys.* **79,** 4694 (1983).
5. L. LEISEROWITZ, *Acta Crystallogr. Sect. B* **32,** 775 (1976).
6. B. H. MEIER, R. MEYER, R. R. ERNST, A. STÖCKLI, A. FURRER, W. HÄLG, AND I. ANDERSON, *Chem. Phys. Lett.* **108,** 522 (1984).
7. B. H. MEIER, R. MEYER, R. R. ERNST, P. ZOLLIKER, A. FURRER, AND W. HÄLG, *Chem. Phys. Lett.* **103,** 169 (1983).
8. W. SCHAJOR, H. POST, R. GROSESCU, U. HAEBERLEN, AND G. BLOCKUS, *J. Magn. Reson.* **53,** 213 (1983).
9. R. FELD, M. S. LEHMANN, K. W. MUIR, AND J. C. SPEAKMAN, *Z. Krist.* **157,** 215 (1981).
10. B. H. MEIER, R. R. ERNST, A. FURRER, A. STÖCKLI, AND I. ANDERSON, unpublished work.
11. A. W. HEWAT, *Nature (London)* **246,** 90 (1973).
12. M. BAILEY AND C. J. BROWN, *Acta Crystallogr.* **22,** 387 (1967).
13. E. STEICHELE AND P. ARNOLD, *Phys. Lett. A* **44,** 165 (1973).

14. J. D. JORGENSEN AND F. J. ROTELLA, *J. Appl. Crystallogr.* **15,** 27 (1982).
15. C. WINDSOR, "Pulsed Neutron Scattering," Taylor & Francis, London (1981).
16. A. W. HEWAT, *Nucl. Instrum. Methods.* **127,** 361 (1975).
17. W. KUHS, *Acta Crystallogr. Sect. A* **39,** 148 (1983).
18. J. M. CARPENTER, G. H. LANDER, AND C. G. WINDSOR, *Rev. Sci. Instrum.* **55,** 1019 (1984).
19. S. R. MACEWEN, J. FABER, JR., AND A. P. L. TURNER, *Acta Metallogr.* **31,** 657 (1983).
20. J. D. JORGENSEN AND J. FABER, JR., *in* "ICANS-VI, Proceedings of the Sixth International Collaboration on Advanced Neutron Sources," pp. 105–114, Argonne National Laboratory, Argonne, Ill. (1983).
21. A. W. HEWAT AND I. BAILEY, *Nucl. Instrum. Methods* **137,** 463 (1976).
22. A. W. HEWAT, "Powder, A Computer Program System for Neutron Powder Diffraction," ILL Internal Report (1977).
23. H. M. RIETVELD, *J. Appl. Crystallogr.* **2,** 65 (1969).
24. A. W. HEWAT, "The Rietveld Program for the Profile Refinement of Atomic and Magnetic Structures—Modified for Anisotropic Thermal Vibration," Harwell Report 73/239 and ILL Report 74/H62S (1973).
25. C. K. JOHNSON, "ORTEP" Report ORNL-3794, Oak Ridge National Laboratory (1965).
26. R. B. VON DREELE, J. D. JORGENSEN, AND C. G. WINDSOR, *J. Appl. Crystallogr. 15,* 581 (1982).
27. E. PRINCE, *J. Appl. Crystallogr.* **14,** 157 (1981).